



# ECC Report <No>

Compatibility analysis (inter-service and intra service) for  
S-PCS below 1 GHz

**approved DD Month YYYY (Arial 9)**

[last updated: DD Month YYYY] (Arial 9)

## 0 EXECUTIVE SUMMARY (STYLE: ECC HEADING 1)

Body text (style: ECC Paragraph)<sup>1</sup>

(advice: the Executive Summary should provide a short and concise explanation on the purpose of the respective ECC Report and should clearly indicate the covered subjects to which it applies. In addition, it should clearly explain the application of the document.)

---

<sup>1</sup> Example of Footnote

## TABLE OF CONTENTS

<b>0</b>	<b>Executive summary (style: ECC Heading 1)</b>	<b>2</b>
<b>1</b>	<b>Introduction</b>	<b>5</b>
<b>2</b>	<b>Definitions (optional section)</b>	<b>6</b>
<b>3</b>	<b>Heading (style: ECC Heading 1)</b>	<b>Error! Bookmark not defined.</b>
3.1	Heading 2 (style: ECC heading 2)	<b>Error! Bookmark not defined.</b>
3.1.1	Heading 3 (style: ECC Heading 3)	<b>Error! Bookmark not defined.</b>
3.1.1.1	Heading 4 (style: ECC Heading 4)	<b>Error! Bookmark not defined.</b>
3.2	Example of bulleted lists	<b>Error! Bookmark not defined.</b>
3.3	Example of numbered lists	<b>Error! Bookmark not defined.</b>
3.4	Example of lettered lists	<b>Error! Bookmark not defined.</b>
3.5	Examples of figures and tables	<b>Error! Bookmark not defined.</b>
<b>4</b>	<b>Conclusions</b>	<b>Error! Bookmark not defined.</b>
<b>ANNEX 1:</b>	<b>Heading (style: ECC Annex - Heading1)</b>	<b>8</b>
<b>ANNEX 2:</b>	<b>Heading (style: ECC Annex - Heading1)</b>	<b>9</b>
<b>ANNEX 3:</b>	<b>List of Reference</b>	<b>10</b>

Note on the Table of Contents (delete after reading)

This is automatically styled and compiled from the headings, subheadings and page numbers from the document that follows. To update the Table of Contents move cursor within the table and press F9.

LIST OF ABBREVIATIONS

Abbreviation	Explanation (style: ECC Table Header red font)
CEPT	European Conference of Postal and Telecommunications Administrations
ECC	Electronic Communications Committee
<abbrev>	<explanation – edit the table as necessary>

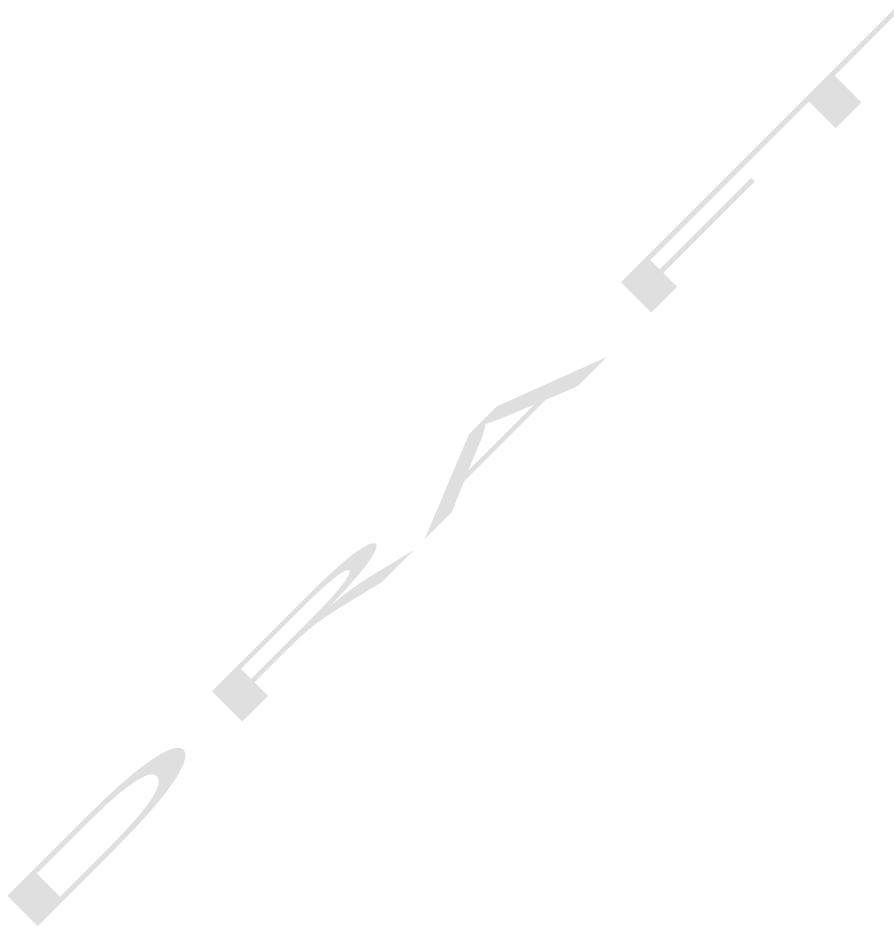
DRAFT

## 1 INTRODUCTION

Body text (style: ECC Paragraph)

(advice: this document gives a template for preparing an ECC Report. All existing contents including the annexes are given for information/formatting purposes only, and shall be replaced by the relevant contents of the new ECC Report.)

Editor's Note 1: This is a note from an editor

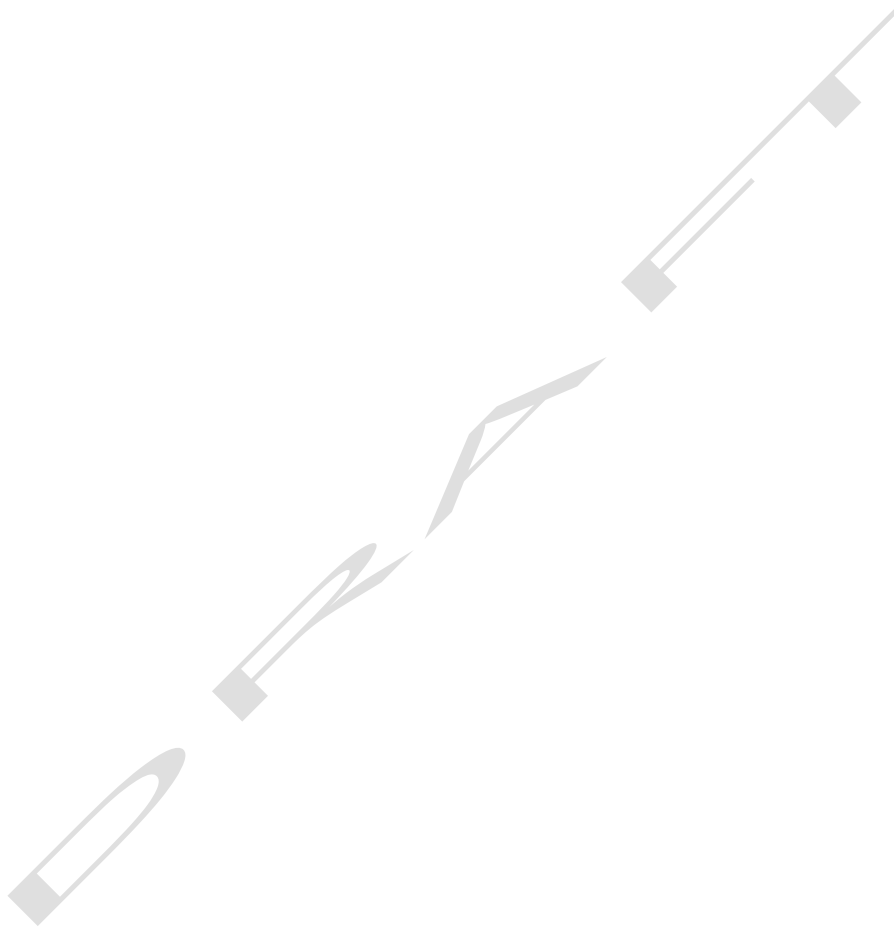


2 DEFINITIONS (OPTIONAL SECTION)

Term	Definition
ECC Table text	ECC Table text
ECC Table text	ECC Table text
ECC Table text	ECC Table text

### 3 INCUMBENT SYSTEMS

[studies are required to consider the protection of existing systems in the meteorological satellite service (space to earth) in the frequency band 137-138]



**ANNEX 1: HEADING (STYLE: ECC ANNEX - HEADING1)**

Body text (style: ECC Paragraph)

**A1.1 HEADING 2 (STYLE: ECC ANNEX HEADING2)**

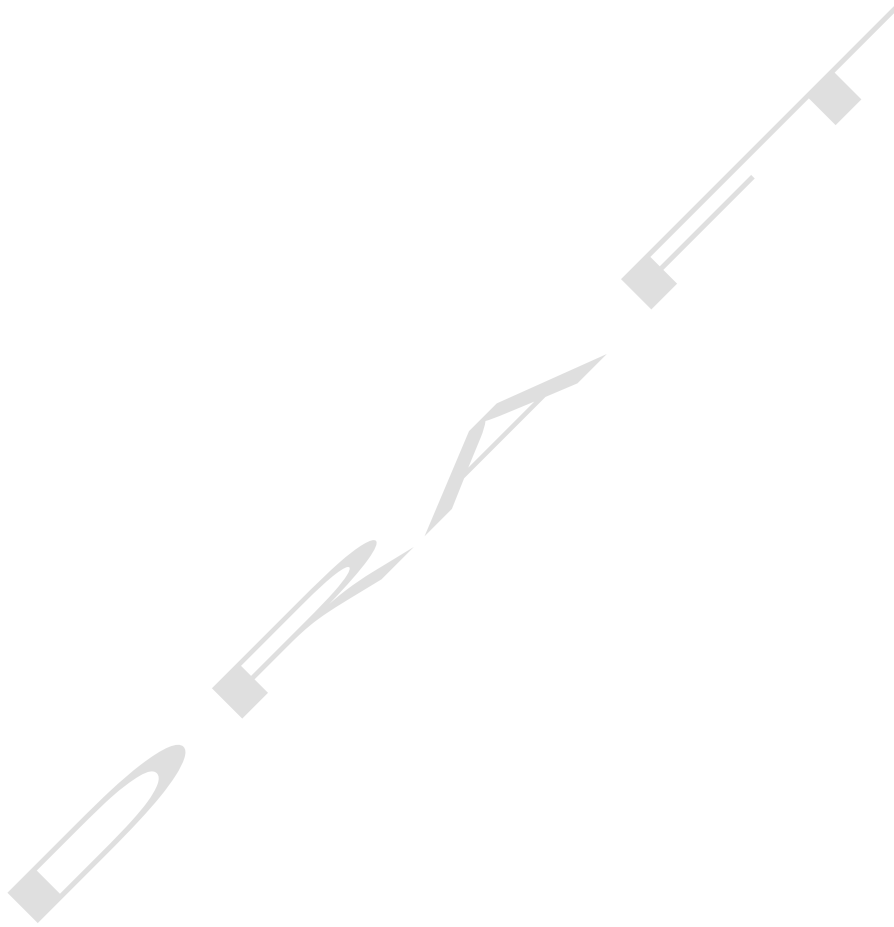
DRAFT



## **ANNEX 2: HEADING (STYLE: ECC ANNEX - HEADING1)**

### **A2.1.1 Heading 3 (style: ECC Annex heading3)**

#### *A2.1.1.1 Heading 4 (style: ECC Annex heading4)*



### ANNEX 3: LIST OF REFERENCE

- [1] Reference one (style: reference)
- [2] Reference two
- [3] etc.

DRAFT

## ANNEX 4: HIBERBAND SYSTEM OVERVIEW



## ANNEX 5: COMPATIBILITY WITH THE RADIO ASTRONOMY SERVICE

### 3.1 INTRODUCTION

The Radio Astronomy Service use of the protected bands 150.05–153 MHz and 406–410 MHz is of high importance for many observatories not only in Europe but all around the world and its protection from terrestrial and space-borne sources must be guaranteed. Among the observatories in Europe (see Table 1), which make observations in these bands, are Jodrell Bank (UK), Effelsberg (Germany), several dozens of LOFAR stations (Netherlands and many CEPT countries), Nançay (France), and Pushchino (Russia). Due to the extreme sensitivity of radio telescopes it is a normal practice to locate them in isolated regions or to look for geographical protection to avoid (as much as possible) the ubiquitous radio frequency interference in populated areas. Being run under public funds, most radio telescopes enjoy the protection of their National Administration when granting licenses to new services that can generate interference in their operations.

The protection of these bands allowed for some famous results such as the 408 MHz all-sky map, which was done with Jodrell, Effelsberg and Parkes (Australia). Effelsberg also participated in measurements of the landing of the NASA Mars-rover mission “Insight” (at a frequency of 400 MHz). The Nançay observatory operates the radio astronomy bands 150–153 MHz and 406–410 MHz with the radio telescopes Radioheliograph and ORFEES for observations of the Sun and for space weather. The 150 MHz band is also used by the LOFAR station located at Nançay observatory. The ORFEES instrument is a spectro-heliograph dedicated for the real-time monitoring of solar activity. The data is used for the study of solar flare as well as for space weather related to the French Air Force.

The Nançay radioheliograph (NRH) produces interferometric images of the Sun's corona in the frequency range 150–450 MHz. It is one of the major telescopes in the world capable of imaging the sun in the VHF range. It plays an important role in the diagnosis of non-thermal emissions from corona, and provides a support service to several space missions, such as STEREO, Parker Solar Probe (PSP) and Solar Orbiter. NRH data can also play an important role in monitoring space weather.

The 150 MHz and 400 MHz frequencies are also extensively used for Pulsar research.

This Annex presents studies of uplink and downlink frequencies of the proposed S-PCS <1GHz to find the necessary separation distance (in the case of uplinks) or to verify the compliance to the requirements established by Rec. ITU-R RA.769 and Res. 739 (in the case of downlink).

**Table 1: List of RAS stations in Europe operating in the 150 MHz and/or the 408 MHz bands.**

Observatory	Country	Geographical latitude	Geographical longitude
Pushchino	Russia	54°49'20" N	37°37'53" E
Jodrell Bank	United Kingdom	53°14'10" N	-02°18'26" E
Westerbork	Netherlands	52°55'01" N	06°36'15" E
LOFAR (core)	Netherlands	52°55' N	06°52' E
Effelsberg	Germany	50°31'32" N	06°53'00" E
Nançay	France	47°22'24" N	02°11'50" E

Medicina	Italy	44°31'14" N	11°38'49" E
Sardinia	Italy	39°29'34" N	09°14'42" E
LOFAR (remote stations)	Poland, Germany, UK, Ireland, Sweden, France, Latvia		

### 3.2 CASES CONSIDERED

The RAS frequency bands considered are 150.05–153 MHz and 406–410 MHz. A number of S-PCS use frequencies adjacent or very close to these two bands. The following cases are relevant:

- TT&C Uplinks in 150 MHz:
  - Hiber system TT&C
- Subscriber uplinks in 150 MHz:
  - LEOTELCOM-1
  - SWARM
- Subscriber downlinks in 150 MHz:
  - SWARM
- Subscriber uplinks in 400 MHz:
  - Hiber
  - Argos
- Subscriber downlinks in 400 MHz:
  - Hiber
  - Kineis

### 3.3 S-PCS SYSTEMS PARAMETERS

Based on the information available, the technical parameters of the satellite systems are collected in the following table.

**Table 2: System parameters of the S-PCS<1GHz under study for up- and downlink.**

	Fo	Ptx	Go	d	B	N	OOB	PSD in RAS band
Hiber TT&C	149 MHz	100W	0 dBi*	10 %*	15 kHz	1	-60 dBc*	-91.8 dBW/Hz
LEOTEL-1 Uplinks	149 MHz	10 dBW/4kHz	0 dBi*	0.01 %	5 kHz	1	-60 dBc*	-126.1 dBW/Hz
SWARM Uplink	149 MHz	10 dBW/4kHz	0 dBi	1%	20.8 kHz	1	-60 dBc*	-106 dBW/Hz
Hiber Uplink	400 MHz	1.5 W	0 dBi*	1.8 %	120 kHz	1	-65 dBc	-131.5 dBW/Hz
Argos	400 MHz	1 W	0 dBi*	0.3 %	120 kHz*	1	-60 dBc*	-136 dBW/Hz

	Fo	Ptx	Go	d	B	N	OOB	PSD in RAS band
Uplink								
SWARM Downlink	137.5 MHz	1.5 W	0 dBi			150	-65 dBc*	-112.4 dBW/Hz
Hiber Downlink	400 MHz	10 W	8 dBi		150 kHz	72		-138 dBW/Hz
Kinéïs Downlink	400 MHz		-3.96 dBi	100%*		25		-140 dBW/Hz

(\*) → Assumption

### 3.4 UPLINKS COMPATIBILITY STUDY

To study the compatibility between a radio telescope and a terrestrial transmitter the propagation model ITU-R P.452-16 is used, this model is recommended for use in compatibility studies from above 0.1 GHz and considers line of sight, diffraction and scatter among other propagation mechanisms. To conduct a generic study a flat terrain is often considered, but the real strength of Rec. P.452 lies in its ability to include propagation loss due to terrain irregularities around specific sites.

The minimum attenuation (or Minimum Coupling Loss, MCL) is obtained as the difference between the average transmitted power in the RAS band and the protection limit defined in Rec. ITU-R 769-2 for each frequency range. Likewise, the minimum distance (so-called separation distance) that is necessary to exceed the MCL is calculated for each system.

#### 3.4.1 Single transmitter case

The study of compatibility between terrestrial transmitters (uplinks) and a RAS station observing in 150.05-153 MHz or 406-410 MHz is described here. The study is conducted considering a single transmitter of which the following characteristics are collected:

**Table 3: Quantities and their physical units relevant to the single-transmitter scenario.**

Parameter	Symbol	Unit
Centre frequency	Fo	MHz
Tx power	Ptx	dBW
Duty cycle	d	%
Channel BW	B	kHz
Number of channels simultaneously used	N	
Tx gain towards RAS station (in the RAS frequency)	G_ras	dBi
Out of Band attenuation	OOB	dBc

The power spectral density radiated in the RAS band can be calculated as:

$$Psd_{tx} = P_{tx} + OOB + G_o + 10 * \log\left(\frac{d}{100}\right) + 10 * \log(N) - 10 * \log(B) \left[\frac{dBW}{Hz}\right]$$

The calculated PSD in the RAS bands is included in Table 2.

The protection limits defined in Rec. ITU-R RA.769-2 are:

$$Psd_{limit_{150MHz}} = -264 \left[\frac{dBW}{Hz}\right]$$

$$Psd_{limit_{408MHz}} = -269 \left[\frac{dBW}{Hz}\right]$$

The minimum coupling loss required is:

$$MCL = Psd_{tx} - Psd_{limit}$$

To obtain the minimum distance necessary between the considered transmitter and a RAS station conducting observations in these frequency bands the propagation model from Rec. ITU-R P.452-16 is used with the following assumptions:

**Table 4: Path propagation parameters for terrestrial sight lines.**

Transmitter height	Htx	2 m
Receiver height	Hrx	2 m
Percentage of time	p	2%
Temperature	290	K
Pressure	1013	hPa
Path profile (*)		
Clutter	UNKNOWN	
Mean Longitude	7	deg
Mean Latitude	50	deg

(\*) To make the studies generic, a flat path is considered. This effectively means that the P452 model will consider effects like: Line of Sight, Diffraction on the spherical Earth surface, Tropo-scatter and Ducting.

With these parameters the following total loss curves are obtained:

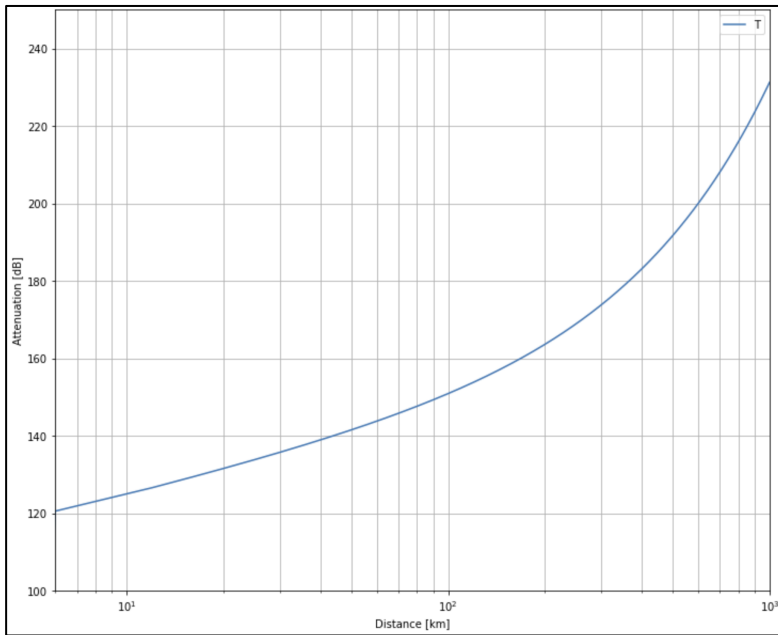


**Figure 1: Total attenuation at 150 MHz.**

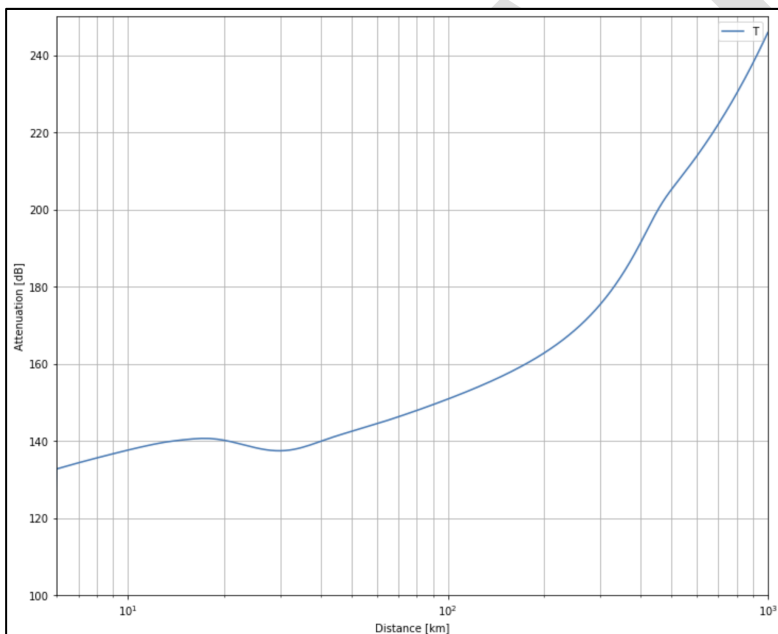


**Figure 2: Total attenuation at 408 MHz.**

Note that the "dip" in the attenuation in Figure 2 (at about 30 km) is caused by anomalous propagation effects.

#### 3.4.1.1 Results

Considering the PSD limit in each band as defined in RA.769, the MCL is calculated and the minimum separation distance is obtained from the figure 1 and 2 graphs.



**Table 5: Results of the terrestrial single-interferer studies.**

	MCL	Minimum separation
HIBER TT&C	172.5 dB	286 km
LEOTEL-1 Uplinks	138.1 dB	38 km
SWARM Uplink	158 dB	153 km
HIBER Uplink	137 dB	10 km
ARGOS Uplink	132 dB	7 km

For a generic study, Table 5 reflects the minimum distance that different system's uplinks need to comply to the RA.769 requirements considering a single transmitter. In many cases, clutter attenuation will apply and the separation distance will be much smaller. However, the single-interferer scenario is usually conducted as a worst-case scenario. For more realistic results, clutter can be included, as well as the distribution of duty cycles, but then, also the deployment densities of the subscribers would need to be taken into account; see next Section [IF NOT REMOVED].

### 3.4.2 Multiple transmitters case

[Note: To be developed, if seen relevant by SE40]

## 3.5 DOWNLINKS COMPATIBILITY STUDY

### 3.5.1 Single transmitter case

[Note: To be developed, if seen relevant by SE40]

### 3.5.2 Aggregated case (equivalent power flux density method)

For satellite constellations of nGSO systems the equivalent-power flux density (EPFD) method as outlined in Recs. ITU-R S.1586 and M.1583 is used. For this, each satellite constellation is fully simulated for a given time period, here 2000 seconds, and the aggregated power flux density (pfd) is determined. As it is possible that certain sky areas have a higher likelihood of being disturbed, M.1583 proposes to split the visible sky (elevations above 0 deg) into cells of approximately equal solid angle and analyse the (cumulative) distribution function of the received aggregated pfd's. Recommendation ITU-R RA.1513 permits other services to interfere with the RAS for 2% of the time. Unfortunately, it is not well laid out, how this criterion is to be understood. One interpretation could be to calculate the 98% percentile level of the received aggregated pfd's over the full sky and compare that number to the threshold value given in Rec. ITU-R RA.769 (hereafter call total data loss). However, other studies in ECC SE40, e.g. of the Iridium constellation, seem to count the number of sky cells in which the average pfd is larger than the RAS threshold and relate that to the total number of cells, i.e., no more than 2% of the sky area must be affected. These analyses were classically performed in the topocentric frame (azimuth and elevation). But radio astronomy almost always observes sources in the equatorial frame, in which stars and other astronomical objects are more or less fixed (in contrast to the topocentric frame, where stars appear to move with time, owing to Earth's

rotation). Therefore, one could also demand that any object in the sky, i.e., a given sky cell in the equatorial frame, must not be affected by RFI for more than 2% of the observing time. This would actually be the approach that fits best to the nature of astronomical observations, where scientists need to propose which astronomical objects are worth to be observed for a given time (these proposal are then reviewed and owing to the limited number of RAS facilities, observing time is often heavily overbooked, such that only a small fraction of proposals is granted time). It would be very ineffective if after such a work-intensive process, the source of interest could only be observed properly for a fraction much smaller than 98% of the time. In the following, the figures of merit for all three approaches are computed.

For the EPFD simulations, the first step is to calculate the satellite positions for a range of time steps. Here, 2000 s were simulated, with a time resolution of 1 s. For a statistical meaningful result, the simulation must be repeated a number of times, such that one can work with the averages over many orbit realizations. With 200 iterations, the performed simulations provided stable results (in the statistical sense). To calculate the aggregate pfd for each iteration, an observer (RAS station) location needs to be defined. Three hypothetical sites were chosen, having geographic latitudes of 0°, 50°, and 80° (the geographical longitude was 0° in all cases). It is also necessary to determine the position of the observer in the moving satellite frame in order to calculate the effective satellite antenna gain towards the observer. Likewise, in the topocentric frame, for a given boresight angle of the radio telescope the angular separation to the apparent position of each satellite must be computed in order to determine the effective RAS antenna gain. This needs to be repeated for each satellite and naturally depends on the observing time.

The next step is to create a grid of sky cells. Annex 1 of Rec. ITU-R M.1583 describes a possible scheme, which is followed here. The size of the cells was chosen to have a solid angle of 1 square degree each. For each iteration and for each sky cell a random RAS pointing position is chosen (which must be located within the sky cell). It is important that these random pointings are uniformly distributed on the sphere, which can be done by sampling the azimuth angle uniformly between the lower and upper boundary of the cell, while the elevation must be sampled according to the following formula:

$$Az_i \sim U(Az_{i,low}, Az_{i,high}),$$

$$El_i \sim 90^\circ - \cos^{-1} U(z_{i,low}, z_{i,high});$$

$$\text{with } z_{i,\{low,high\}} = \cos(90^\circ - El_{i,\{low,high\}}).$$

In Table 6 to Table 8 the results for the satellite systems are summarized for each of the simulated observer latitudes. Furthermore, in Figure 3 to Figure 7 (for the example of the Hiber system) the results for each sky cell is visualized, showing the aggregated pfd (i.e., summed over all satellites and averaged with respect to the 2000 s integration time) received in each cell (displayed is the average of all iterations) and the data loss per cell for both the topocentric and equatorial frames. Based on the former it is possible to count the ratio of cells, where the average pfd is higher than the permitted threshold. Furthermore, for all systems under study one finds a number of grid cells in the equatorial frame where the data loss is larger than 2%, which would significantly affect the observing possibilities for astronomical objects in such sky areas. However, Rec. ITU-R RA.1513 allows all services together to pollute up to 5% of the data. If the different constellations would affect mostly different sky cells one could possibly accept a maximum data loss of up to 5% per equatorial cell even for an individual service. This is subject to further studies.

**Table 6: Results for RAS station latitude of 0°.**

	Total data loss	Fraction of bad cells	Number of cells with more than 2% loss (equatorial)	Number of cells with more than 5% loss (equatorial)
LEOTEL-1 Downlinks				
SWARM Downlinks	100%	100%	40626	40626

	Total data loss	Fraction of bad cells	Number of cells with more than 2% loss (equatorial)	Number of cells with more than 5% loss (equatorial)
HIBER Downlinks	1.41%	0.01%	4434	169
ARGOS Downlinks	0.73%	0%	1207	8

(Total number of simulated equatorial-grid sky cells: 40626)

**Table 7: Results for RAS station latitude of 50°.**

	Total data loss	Fraction of bad cells	Number of cells with more than 2% loss (equatorial)	Number of cells with more than 5% loss (equatorial)
LEOTEL-1 Downlinks				
SWARM Downlinks	100%	100%	30938	30938
HIBER Downlinks	2.15%	0.1%	7807	1304
ARGOS Downlinks	1.21%	0%	3317	171

(Total number of simulated equatorial-grid sky cells: 30938)

**Table 8: Results for RAS station latitude of 80°.**

	Total data loss	Fraction of bad cells	Number of cells with more than 2% loss (equatorial)	Number of cells with more than 5% loss (equatorial)
LEOTEL-1 Downlinks				
SWARM Downlinks	100%	100%	20626	20626
HIBER Downlinks	10.36%	19.6%	17186	13941
ARGOS Downlinks	3.25%	0.17%	9974	3820

(Total number of simulated equatorial-grid sky cells: 20626)

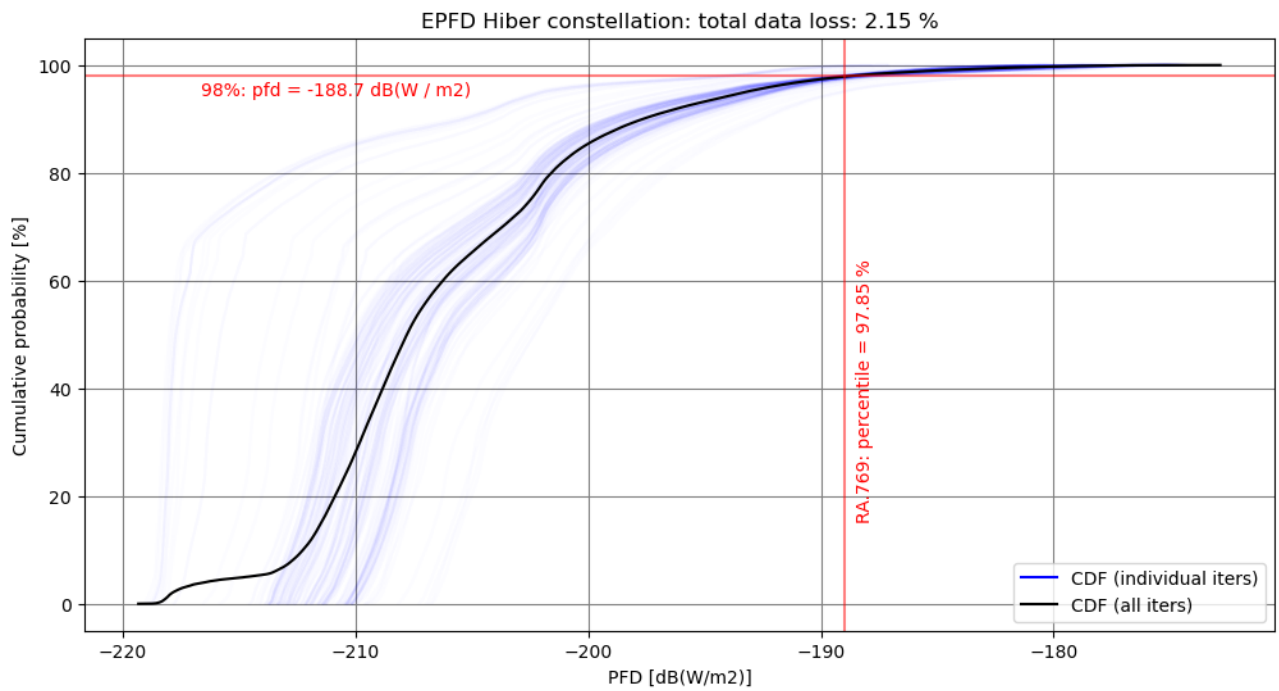


Figure 3: Cumulative distribution function for epfd values (observer @ 50° latitude).

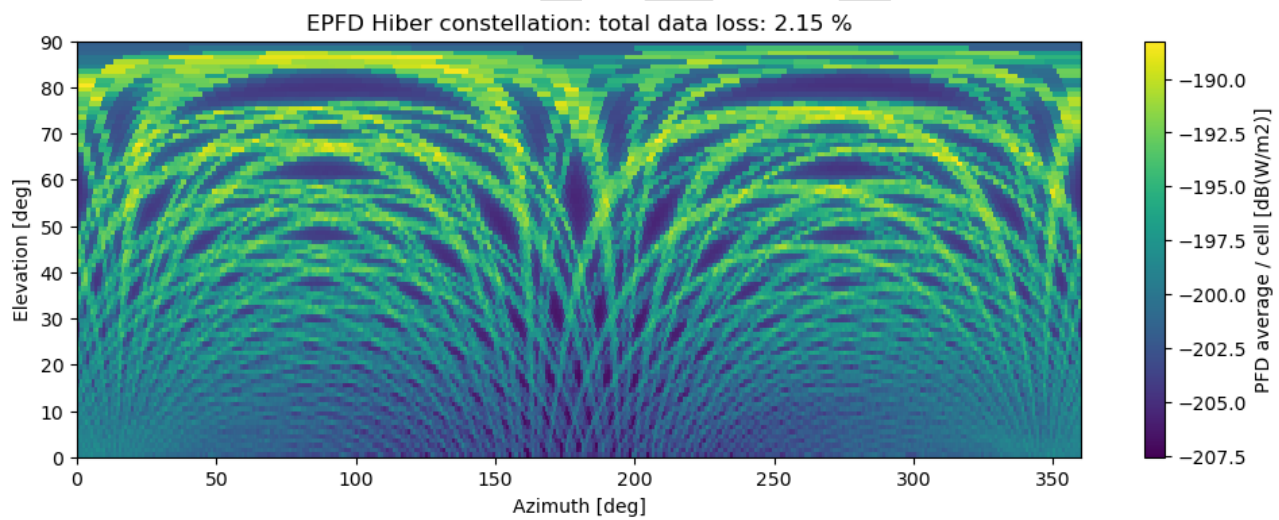


Figure 4: Average epfd for each simulated sky cell in the horizontal frame (observer @ 50° latitude).

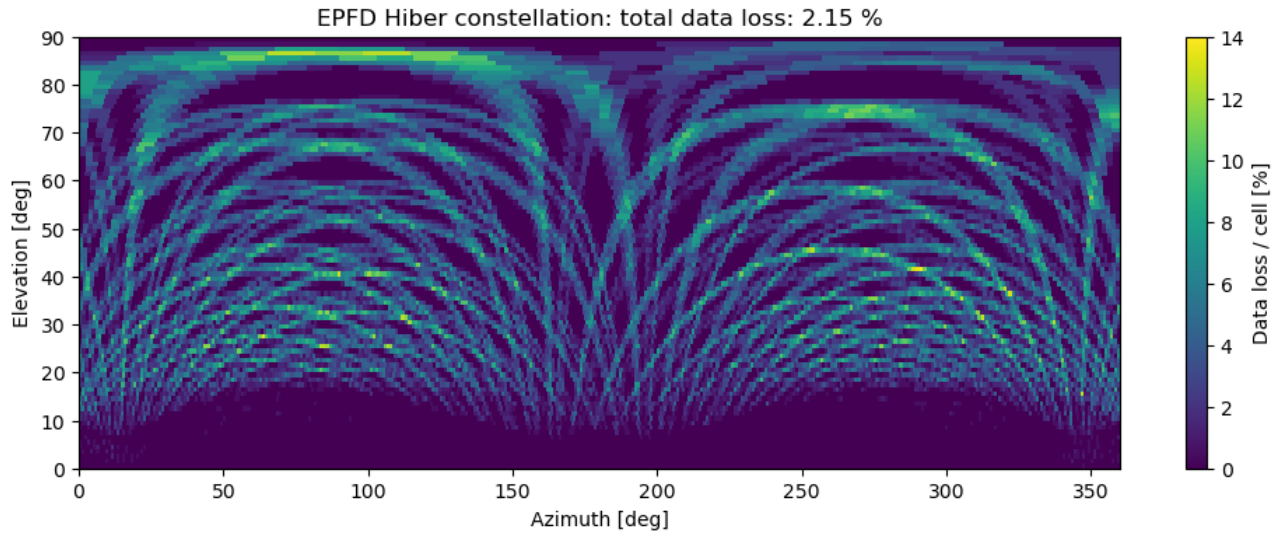


Figure 5: Data loss rate for each simulated sky cell in the horizontal frame (observer @ 50° latitude).

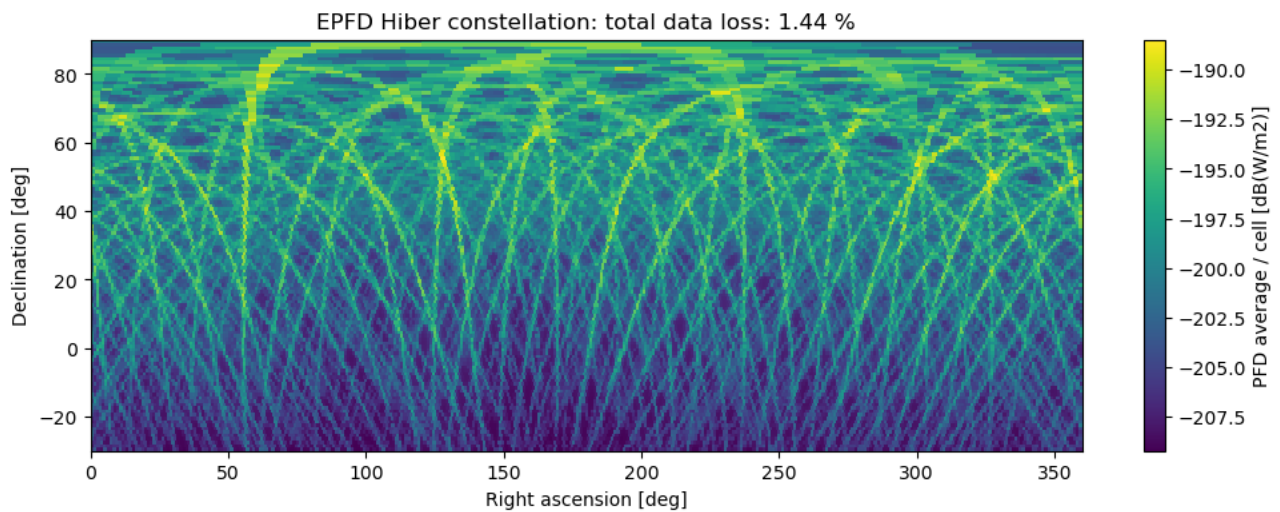


Figure 6: Average epfd for each simulated sky cell in the equatorial frame (observer @ 50° latitude).

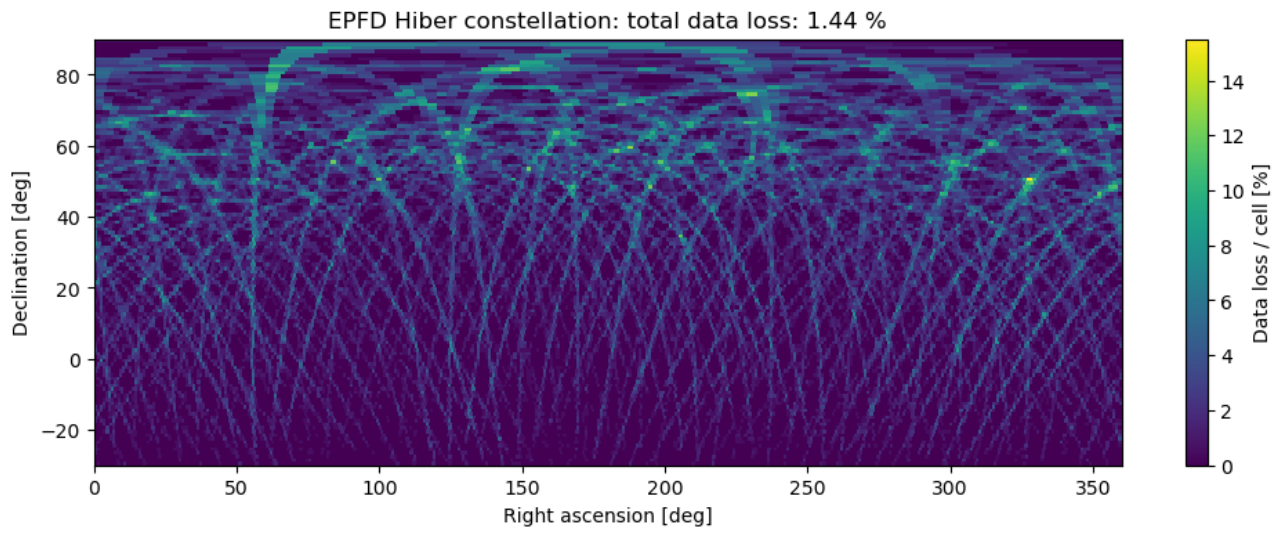


Figure 7: Data loss rate for each simulated sky cell in the equatorial frame (observer @ 50° latitude).